MorphMLP: A Self-Attention Free, MLP-Like Backbone for Image and Video

David Junhao Zhang[1*†] Kunchang Li[3, 4*] Yunpeng Chen[2] Yali Wang[3]
Shashwat Chandra[1] Yu Qiao[5] Luoqi Liu[2] Mike Zheng Shou[1]

[1]National University of Singapore [2]Meitu, Inc
[3]Shenzhen Institutes of Advanced Technology, Chinese Academy of Sciences
[4]University of Chinese Academy of Sciences [5]Shanghai AI Laboratory

Abstract

Self-attention has become an integral component of the recent network architectures, e.g., Transformer, that dominate major image and video benchmarks. This is because self-attention can flexibly model long-range information. For the same reason, researchers make attempts recently to revive Multiple Layer Perceptron (MLP) and propose a few MLP-Like architectures, showing great potential. However, the current MLP-Like architectures are not good at capturing local details and lack progressive understanding of core details in the images and/or videos. To overcome this issue, we propose a novel MorphMLP architecture that focuses on capturing local details at the low-level layers, while gradually changing to focus on long-term modeling at the high-level layers. Specifically, we design a Fully-Connected-Like layer, dubbed as MorphFC, of two morphable filters that gradually grow its receptive field along the height and width dimension. More interestingly, we propose to flexibly adapt our MorphFC layer in the video domain. To our best knowledge, we are the first to create a MLP-Like backbone for learning video representation. Finally, we conduct extensive experiments on image classification, semantic segmentation and video classification. Our MorphMLP, such a self-attention free backbone, can be as powerful as and even outperform self-attention based models.

1. Introduction

Since the seminal work of Vision Transformer (ViT) [14], self-attention based architectures have been pushing the envelope in a variety of computer vision tasks: **(i) Image domain**: several works [13, 40, 67, 76] make remarkable progress on enabling Transformer architecture to become a general backbone on many downstream image tasks.

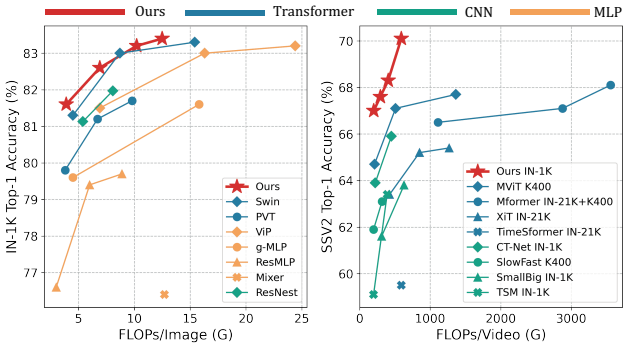

Figure 1. Comparisons between our MorphMLP and other state-of-the-art Transformer, CNN and MLP-Like methods. Left: ImageNet-1K [12]; Right: Something-Something V2 [22].

(ii) Video domain: a couple of methods [3, 36, 42, 47, 48] explore space-time self-attention for video understanding, achieving amazing performance. We conjecture that the effectiveness of Transformer thanks to the self-attention layer, which can dynamically capture long-range dependencies. However, an interesting question has been raised: *Is self-attention a must-have?*

Convolutional Neural Network (CNN) is a popular self-attention free architecture. Typical convolutional operators (e.g., 3×3 convolution) excel at capturing local structure. Yet, CNN is not good at modeling long-term dependencies. To tackle this problem, a couple of methods [9, 29, 68, 80] integrate self-attention mechanism to obtain long-range information. Such methods still rely on self-attention to supplement local features and boost performance.

Alternatively, researchers recently have made attempts to replace self-attention with Multiple Layer Perceptron (MLP) because the Fully-Connected (FC) layer can also model the long-term dependencies. Surprisingly, such MLP-Like architecture [8, 25, 39] can achieve comparable results with Transformers, which indicates that self-attention may not be a must-have. Yet, there are two critical challenges for SOTA MLP-Like models: **(i) Cannot cope**

*David J. Zhang and K. Li contribute equally.
†Work is done during internship at Meitu, Inc.

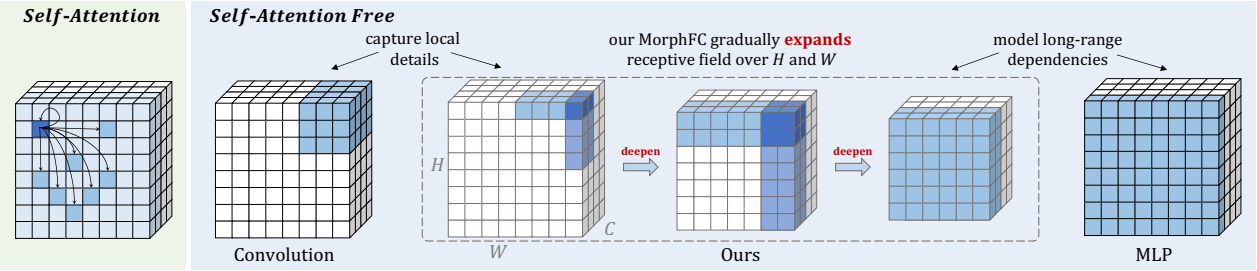

Figure 2. Overview of self-attention, convolution, MLP-Like and our architecture.

with different scale images. Because the number of parameters in their FC layers is fixed and equal to originally input image size H×W. **(ii) Inferior performance due to overlooking local details**. Like in ViP [25], even at the low-level layers, the receptive field of each filter spans a long range, making it difficult to learn to capture local details. Furthermore, this makes MLP-Like architectures not suitable for dense prediction, e.g., semantic segmentation which requires fine-grained local features.

To tackle the above issues of MLP-Like architectures, we propose a simple yet effective self-attention free architecture named MorphMLP as shown in Fig. 2. MorphMLP consists of a stack of novel `MorphFC` layers. At the low-level layers, our `MorphFC` acts similarly to Convolution or window-wise self-attention, capturing local details. As going deeper, our `MorphFC` gradually changes to being similar to the conventional MLP and focusing on long-range information.

Specifically, for each `MorphFC` layer, we split the input tokens along horizontal and vertical directions into chunks (each group of blue grids in Fig. 2) according to the predefined length. We pass each chunk using a conventional FC filter to get a new chunk of the same size. As the network goes deeper, we gradually expand the chunk length. Each `MorphFC` layer has two separate pathways that one's chunk length grows larger in height while another pathway's chunk length grows larger in width, and these two pathways do not share the FC filter's weights. Finally, at the high-level layers, the chunk covers the whole spatial region and thus excels at modeling long-range dependencies. Such hierarchical expansions enable MorphMLP to **capture short-to-long range information**.

This design also resolves the aforementioned issue of fixed input size. Similar to that the number of parameters in convolution filters is decided by window size, the number of parameters in our FC filter is determined by chunk size instead of input image size. Therefore, our MorphMLP can cope with multi-scale images.

In this paper, we take a step further to extend our MorphMLP from image to video. To our best knowledge, **this is the first self-attention free, MLP-Like backbone architecture in the video domain**. Specifically, in addition to the horizontal and vertical pathways, we introduce another temporal pathway to capture long-term temporal information in videos, which concatenates the features from the same spatial locations across all frames into a chunk. Meanwhile, each chunk is processed by the FC filter to get a new chunk of the same size. Based on the new `MorphFC` layer, we extensively explore various ways of building up the backbone for video. Through experiments, we decide to model the spatial and temporal information sequentially to efficiently learn spatial-temporal representation.

As shown in Fig. 1, our MorphMLP achieves outstanding results. This indicates that self-attention free architecture can perform as well as and even outperform self-attention based model.

We summarize our contributions as follows:

- We propose the `MorphFC`, which focuses on local details in early layers, while the network deepens, gradually changes to model long-range information, overcoming the issues of the current CNN and MLP-Like models.
- We extend our MorphMLP to video recognition and set new state-of-the-art results. To the best of our knowledge, this is the first MLP-Like video backbone.
- MorphMLP can achieve state-of-the-art performance on image classification, semantic segmentation and video classification tasks including ImageNet-1K [12], Something-Something V1&V2 [22], Kinetics400 [6] and ADE20K datasets [78].
- Given the strong performances of our method, we shed light on studying whether self-attention is a must-have or a manner of capturing local details and long-range dependencies might be more important. These results demonstrate that the self-attention free model can be as powerful as self-attention based architecture and show the great potential that MLP-Like architecture can become a new paradigm of versatile backbone.

2. Related Work

Self-Attention based backbones. Vision Transformer (ViT) [14] firstly applies Transformer architecture to a sequence of image tokens. It utilizes multi-head self-attention

to capture long-range dependencies, thus achieving amazing results on image classification. Following works [13, 40, 53, 67, 70, 76] make a series of breakthroughs to achieve state-of-art performance on several image tasks, i.e., semantic segmentation [31, 72] and object detection [5, 79]. In video domain, a couple of woks [3, 16, 36, 42, 48, 74] explore space-time self-attention to model spatial-temporal relation and achieve state-of-the-art performance. It seems that self-attention based architectures have been gradually dominating the computer vision community.

In this paper, we aim to explore a simple yet effective self-attention free architecture, which builds upon the FC layer to extract features. Our comparisons show that MorphMLP can outperform Transformers in essential vision applications, indicating that self-attention is not critical.

CNN based backbones. CNNs [26, 27, 49, 51, 73] have dominated vision tasks in the past few years. In image domain, beginning with AlexNet [33], more effective and deeper networks, VGG [52], GoogleNet [54], ResNet [24], DenseNet [28] and EfficentNet [55] are proposed and achieve great success in computer vision. In the video domain, several works [7, 19, 60, 62] explore how to utilize convolution to learn effective spatial-temporal representation. However, the typical spatial and temporal convolution are so local that they struggle to capture long-range information well even if stacked deeper. A series of works propose efficient modules (e.g., Non-local [68], Double Attention [9]) to enhance local features via integrating long-range relation. The improvement of these methods can not be achieved without the supplement of self-attention layers.

In contrast, we propose the `MorphFC`, which is self-attention free but can capture short-to-long range information by progressively adding the length of chunks as the network goes deeper.

MLP-Like based backbones. Recent works [39, 58, 75] try to replace self-attention layer with FC layer to explore the necessity of self-attention in Transformer architecture. But they suffer from dense parameters and computation. [23, 25, 56] apply FC layer along horizontal, vertical, and channel directions, respectively, in order to reduce the number of parameters and computation cost. However, the parameters of FC layer are still determined by the input resolution, so it is hard to handle different image scales. CycleMLP [8] addresses such problem with padding, but it only focuses on global information, ignoring local inductive bias. Meanwhile, the ability of MLP-Like architecture for temporal modeling has not been explored.

On the contrary, our MorphMLP can cope with diverse scales via splitting the sequence of tokens into chunks. Furthermore, it is able to effectively capture local to global information by gradually expanding chunk length. More importantly, we are the first to extend MLP-Like architecture on videos to explore its generalization ability as a new paradigm of versatile backbone.

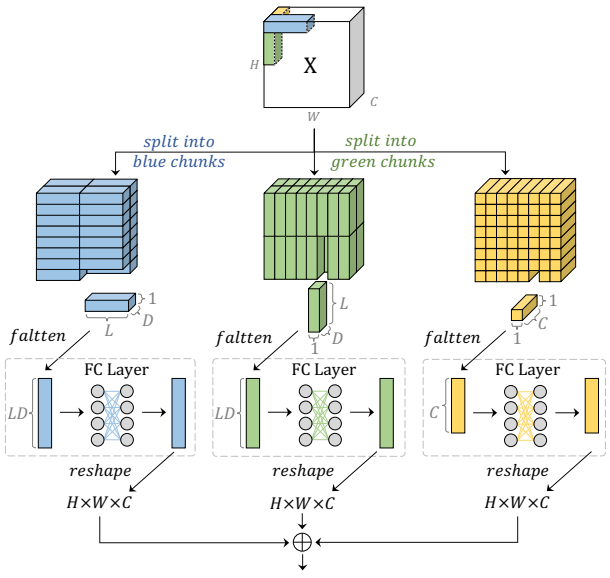

Figure 3. Our `MorphFC` Layer.

3. Method

3.1. MorphMLP in the Image Domain

MorphFC layer. As discussed above, typical CNN and previous MLP-Like architectures only focus on either local or global information modeling. Moreover, the number of parameters of current MLP-Like architecture is determined by fixed image size, which makes it difficult to handle different image resolutions. Motivated by the window used in convolution, we propose a novel `MorphFC` layer to address the above two issues. Our `MorphFC` processes the image tokens in horizontal and vertical pathways. We take the horizontal one (blue chunks in Fig. 3) for example.

Specifically, given an input image $\mathbf{X} \in \mathbb{R}^{H\times W\times C}$ that has been projected into a sequence of image tokens, we first split $\mathbf{X}$ along horizontal direction. We set chunk length to L and thus obtain $\mathbf{X}_i \in \mathbb{R}^{L\times C}$, where $i \in \{1, ..., HW/L\}$. Furthermore, to reduce computation cost, we also split each $\mathbf{X}_i$ into multiple groups along channel dimension, where each group has D channels. To this point, we get split chunks and each single chunk is $\mathbf{X}_i^k \in \mathbb{R}^{LD}$, where $k \in \{1, ..., C/D\}$. Next, we flatten each chunk into 1D vector and apply a FC weight matrix $\mathbf{W} \in \mathbb{R}^{LD\times LD}$ to transform each chunk, yielding

$$\mathbf{Y}_i^k = \mathbf{X}_i^k \mathbf{W}. \tag{1}$$

After feature transformation, we reshape all chunks $\mathbf{Y}_i^k$ back to the original dimension $\mathbf{Y} \in \mathbb{R}^{H\times W\times C}$. The vertical way (green chunks in Fig. 3) does likewise except splitting the sequence of image tokens along vertical direction. To make communication among groups along channel dimension, we also apply a FC layer to process each image

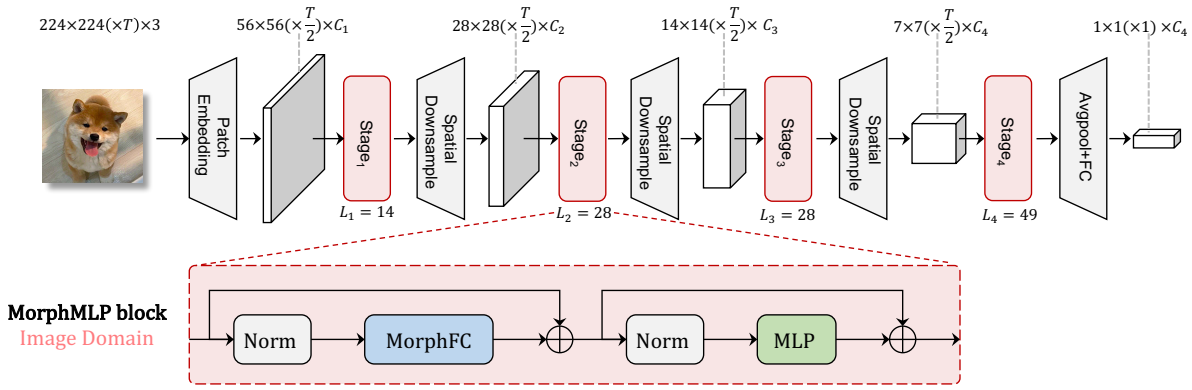

Figure 4. Architecture of our MorphMLP and detailed designs of MorphMLP block in the image domain. L means chuck length.

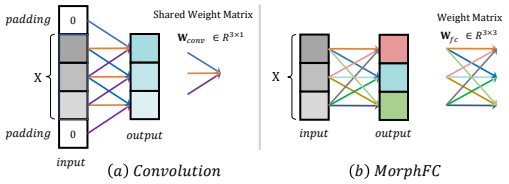

Figure 5. Comparison between 1D convolution and our `MorphFC`.

token individually. Finally, we get the output by element-wise summing horizontal, vertical, and channel features together. The chunks lengths hierarchically increase as the network deepens, aiming at capturing short-to-long range information progressively.

Difference between our MorphFC and convolution. (i) Typical convolution utilizes fixed 3×3 kernel size, which only aggregates local context. On the contrary, the chunks lengths in `MorphFC` hierarchical increase as the network deepens, which can model short-to-long range information progressively. Obviously, the kernel size for 2D convolution can also be set larger but its computation cost is much higher than `MorphFC`.

(ii) Convolution uses sliding windows to obtain overlapping tokens, which requires cumbersome operations, including unfold, reshape and fold. In contrast, we simply reshape the feature map to obtain our chunks with non-overlapping tokens.

(iii) As shown in Fig. 5, given a 1×3 input, to get the 1×3 output, the convolution kernel of 1×3 window size needs to slide three times, and each 1×1 output is generated by the shared weight matrix $\mathbf{W}_{conv} \in \mathbb{R}^{3\times1}$. In contrast, FC layer applies weight matrix $\mathbf{W}_{fc} \in \mathbb{R}^{3\times3}$ to the input yielding 1×3 ouput. Each 1×1 output is equivalent to being generated by non-shared weight matrix $\mathbf{W} \in \mathbb{R}^{3\times1}$, which brings more flexible spatial encoding than convolution. We show the quantitative comparisons in Table 10.

MorphMLP block in the image domain. As shown in Fig. 4, we follow [63] to construct a MorphMLP block by replacing the standard multi-head attention (MSA) module in the Transformer block with `MorphFC`, and the other

Detail	Tiny	Small	Base	Large
Stoch. Dep.	0.1	0.1	0.3	0.4
Depth	3, 4, 7, 3	3, 4, 9, 3	4, 6, 15, 4	4, 8, 18, 6
Channel	84, 168, 336, 588	112, 224, 392, 784		
Chunk Len	14, 28, 28, 49			
#Param.	23M	38M	58M	76M
GFLOPs	3.9	7.0	10.2	12.5

Table 1. Model settings for different variants. A larger stochastic depth rate is set for larger models. All models share the same chunk lengths but different channel numbers and depth.

layers remain unchanged. Within the MorphMLP block, LayerNorm (LN) [2] is applied before `MorphFC` and MLP module, `MorphFC` is followed by GELU activation function, residual connection [24] is used after `MorphFC` and MLP module.

Network architecture. For image recognition, as shown in Fig. 4, we hierarchically stack MorphMLP blocks to build up our network. Given an image $\mathbf{X} \in \mathbb{R}^{H\times W\times3}$, taking H=W=224 for example, our MorphMLP backbone first performs patch embedding on image and gets a sequence of tokens with dimension 56×56×C_1. Then, we have four sequential stages and each of them contains a couple of MorphMLP blocks. The feature size remains unchanged as passing through layers inside the same stage. At the end of each stage excluding the last one, we expand the channel dimension and downsample the spatial resolution of features by ratio 2.

Note that we set chunk lengths of `MorphFC` to be 14, 28, 28, 49 for stage 1-4, respectively. Horizontal/vertical chunks with lengths 14, 28, 28, 49 of stage 1-4 can cover quarter, one, two, all rows/columns of feature maps of stage 1-4, respectively. In shallow layers, our network can learn detailed representation from the local spatial context in small chunk length, e.g., length 14 for 56×56×C_1 feature map. In deep layers, our network can capture long-range information from the global semantic context in considerable chunk length, e.g., length 49 for 7×7×C_4 feature map. By downsampling the spatial resolution and expand-

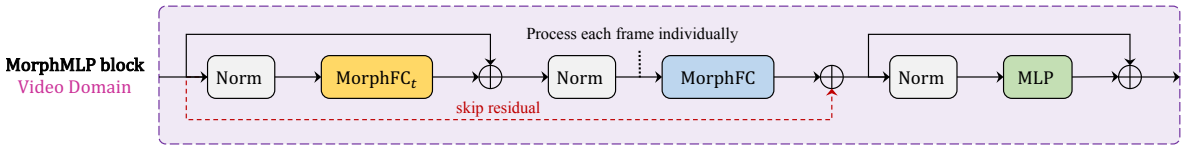

Figure 6. Detailed designs of MorphMLP block in the video domain.

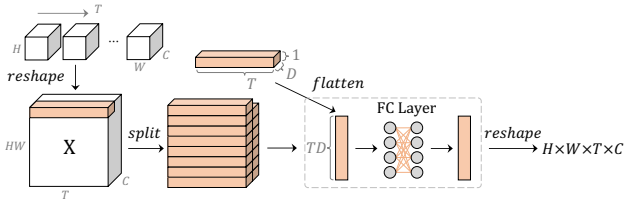

Figure 7. MorphFC$_t$. Extension on temporal dimension.

ing chunk length progressively as the network goes deeper, our MorphMLP is capable of modeling short-to-long range information efficiently.

As shown in Table 1, we provide four model variants including MorphMLP-Tiny(T), Small(S), Base(B) and Large(L).

3.2. MorphMLP in the Video Domain

Extension on temporal dimension. To extend our MorphMLP for temporal modeling, in addition to the horizontal and vertical pathways in MorphFC, we introduce another temporal pathway MorphFC$_t$ to capture long-term temporal information. Specifically, as shown in Fig. 7, given an input video clip tokens $\mathbf{X} \in \mathbb{R}^{H\times W\times T\times C}$, we first split X into a couple of groups along channel dimension (D channels in each group) to reduce computation cost and get $\mathbf{X}^k \in \mathbb{R}^{H\times W\times T\times D}$, where $k \in \{1, ..., C/D\}$. For each spatial position s, we concatenate features across all frames into a chunk $\mathbf{X}_s^k \in \mathbb{R}^{TD}$, where $s \in \{1, ..., HW\}$. Then we apply a FC matrix $\mathbf{W} \in \mathbb{R}^{TD\times TD}$, to transform temporal features and get

$$\mathbf{Y}_s^k = \mathbf{X}_s^k \mathbf{W}. \quad (2)$$

Finally, we reshape all chunks $\mathbf{Y}_s^k \in \mathbb{R}^{TD}$ back to original video clips tokens dimension and output $\mathbf{Y} \in \mathbb{R}^{H\times W\times T\times C}$.

MorphMLP block in the video domain. We propose a factorized spatial-temporal MorphMLP block in the video domain for efficient video representation learning. As shown in Fig. 6, our MorphMLP block in the video domain contains MorphFC$_t$, MorphFC and MLP [63] modules in a sequential order. As indicated in [3], it is difficult for joint spatial-temporal optimization. Therefore, we place temporal and spatial MorphFC layers in the sequential style. The LN [2] layer is applied before each module, and the standard residual connections are used after MorphFC$_t$ and MLP module. Instead of applying a standard residual connection [24] after MorphFC, we add a skip residual connection (red line) between the original input and output features from MorphFC layer. We found that such connection can make training more stable.

	Method	#Param.(M)	GFLOPs	ImageNet Top-1
Self-Attention Based				
Trans	DeiT-S [59]	22	4.6	79.8
	DeiT-B [59]	86	17.5	81.8
	PVT-S [67]	25	3.8	79.8
	PVT-M [67]	44	6.7	81.2
	PVT-L [67]	61	9.8	81.7
	Swin-T [40]	29	4.5	81.3
	Swin-S [40]	50	8.7	83.0
	Swin-B [40]	88	15.4	83.3
Trans + CNN	BoT-S1-50 [53]	21	4.3	79.1
	BoT-S1-59 [53]	34	7.3	81.7
	CvT-13 [71]	20	4.5	81.6
	CvT-21 [71]	32	7.1	82.5
	CONTAINER-L [20]	20	3.2	82.0
	CONTAINER [20]	22	8.1	82.7
	CoAtNet-0 [11]	23	4.2	81.6
	CoAtNet-1 [11]	42	8.4	83.3
Self-Attention Free				
CNN	ResNet50 [24]	26	4.1	78.5
	ResNet101 [24]	45	7.9	79.8
	RegNetY-4 [49]	21	4.0	80.0
	RegNetY-8 [49]	39	8.0	81.7
	ResNest50 [77]	28	4.3	80.6
	ResNest101 [77]	48	8.0	82.0
MLP-Like	Mixer-B/16 [57]	59	12.7	76.4
	ResMLP [58]	116	23.0	81.0
	gMLP-S [39]	20	4.5	79.6
	gMLP-B [39]	75	15.8	81.6
	ViP-S [25]	25	6.9	81.5
	ViP-M [25]	55	16.3	82.7
	MorphMLP-T	23	3.9	81.6
	MorphMLP-S	38	7.0	82.6
	MorphMLP-B	58	10.2	83.2
	MorphMLP-L	76	12.5	**83.4**

Table 2. Comparisons with the state-of-the-art on ImageNet [12]. Our self-attention free MorphMLP can achieve competitive results with and even outperform recent state-of-the-art self-attention based architectures.

Network Architecture. Compared with the network architecture in the image domain, we just need to simply replace the MorphMLP block in the image domain (Fig. 4) with the video domain (Fig. 6) to build up our network for video. For the temporal dimension, the number of frames T is downsampled by ratio 2 in the patch embedding layer. It remains unchanged until the average pooling layer, which is at the end of the network.

4. Experiment

In this section, we first examine the performance of MorphMLP for ImageNet-1K [12] image classification. Then

Method	Pretrain	#Frame	GFLOPs	K400 Top-1	K400 Top-5
Self-Attention Free – CNN					
SlowFast R101 [19]	-	(16+64)×3×10	6390	78.9	93.5
CorrNet-101 [64]	-	32× 3×10	6720	79.2	-
ip-CSN [61]	Sports1M	32× 3×10	3264	79.2	93.8
X3D-XL [18]	-	16×3×10	1452	79.1	93.9
SmallBig$_{EN}$ [35]	IN-1K	(8+32)×3×4	5700	78.7	93.7
TDN$_{EN}$ [65]	IN-1K	(8+16)×3×10	5940	79.4	94.4
CT-Net$_{EN}$ [34]	IN-1K	(16+16)×3×4	2641	79.8	94.2
Self-Attention Based – Transformer					
Timesformer-L [3]	IN-21K	96×3×1	7140	80.7	94.7
VidTr-L [36]	IN-21K	32×3×10	11760	79.1	93.9
ViViT-L [1]	IN-21K	16×3×4	17357	80.6	94.7
X-ViT [4]	IN-21K	16×3×1	850	80.2	94.7
Mformer [48]	IN-21K	32×3×10	11085	80.2	94.8
Mformer-L [48]	IN-21K	32×3×10	35550	80.2	94.8
MViT-B,16×4 [16]	-	16×1×5	355	78.4	93.5
MViT-B,32×3 [16]	-	32×1×5	850	80.2	94.4
VideoSwin-T [42]	IN-1K	32×3×4	1056	78.8	93.6
VideoSwin-B [42]	IN-1K	32×3×4	3384	80.6	94.6
Self-Attention Free – MLP-Like					
MorphMLP-S	IN-1K	16×1×4	268	78.7	93.8
MorphMLP-S	IN-1K	32×1×4	532	79.7	94.2
MorphMLP-B	IN-1K	16×1×4	392	79.5	94.4
MorphMLP-B	IN-1K	32×1×4	788	**80.8**	**94.9**

Table 3. Comparisons with the state-of-the-art on Kinetics-400 [6]. Our MorphMLP outperforms recent state-of-the-art methods with much fewer computation costs.

we verify its effectiveness of spatial-temporal modeling on Kinetics-400 [6], and Something-Something V1&V2 [22]. Moreover, we demonstrate its strong ability in dense prediction tasks, e.g., semantic segmentation on ADE20K [78].

4.1. Image Classification on ImageNet-1K

Settings. We train our models from scratch on the ImageNet-1K dataset [12], which consists of 1.2M training images and 50K validation images from 1,000 categories. Our code is implemented based on `DeiT` [59] repository, and we follow the same training strategy proposed in DeiT [59], including strong data augmentation and regularization. Different stochastic depth rates are set for our different model variants as shown in Table 1. We adopt AdamW [44] optimizer with cosine learning rate schedule [45] for 300 epochs, while the first 20 epochs are used for linear warm-up [21]. The total batch size, weight decay, and initial learning rate are set to 1024, 5×10^{-2} and 0.01 respectively.

Results. (i) Comparisons with self-attention free architectures. As shown in Table 2, our MorphMLP outperforms the state-of-the-art CNN and MLP-Like architectures. Compared with ViP-S [25], our method can get much higher accuracy (82.6% *vs*. 81.5%) with similar GFLOPS (7.0G *vs*. 6.9G). This demonstrates the effectiveness of our progressively short-to-long range pattern.

(ii) Comparisons with self-attention based architectures. In Table 2, our MorphMLP can achieve competitive results with popular self-attention based models. Compared with other tiny models, e.g., Swin-T [40], our method can achieve better results (81.6% *vs*. 81.3%) with fewer parameters and GFLOPS (23M *vs*. 29M, 3.9G *vs*. 4.5G). As for larger settings, our method also outperforms Swin-B [40] (83.4% *vs*. 83.3%) with lower computation (12.5G *vs*. 15.4G). Even compared with hybrid models which consist of self-attention and convolution, our method can still surpass them or achieve comparable results. These results show that without spatial interaction dynamically parameterized by self-attention, our self-attention free `MorphFC` with static parameters can still achieve better results.

Method	Pretrain	#Frame	GFLOPs	SSV2 Top-1	SSV2 Top-5
Self-Attention Free – CNN					
SlowFast R50 [19]	K400	(8+32)×3×1	197	61.7	46.6
TSM [38]	K400	16×3×2	374	63.4	88.5
STM [30]	IN-1K	16×3×10	1995	64.2	89.8
bLVNet [17]	IN-1K	32×3×10	3870	65.2	90.3
TEA [37]	IN-1K	16×3×10	2100	65.1	-
CT-Net [34]	IN-1K	16×3×2	450	65.9	90.1
Self-Attention Based – Transformer					
Timesformer [3]	IN-21K	16×3×1	5109	62.5	-
VidTr-L [36]	IN-21K+K400	32×3×10	10530	60.2	-
ViViT-L [1]	IN-21K+K400	16×3×4	11892	65.4	89.8
X-ViT [4]	IN-21K	32×3×1	1269	65.4	90.7
Mformer [48]	IN-21K+K400	16×3×1	1110	66.5	90.1
Mformer-L [48]	IN-21K+K400	32×3×1	3555	68.1	91.2
MViT-B,16×4 [16]	K400	16×3×1	510	67.1	90.8
MViT-B,32×3 [16]	K400	32×3×1	1365	67.7	90.9
MViT-B-24,32×3 [16]	K600	32×3×1	708	68.7	91.5
Self-Attention Free – MLP-like					
MorphMLP-S	IN-1K	16×3×1	201	67.1	90.9
MorphMLP-S	IN-1K	32×3×1	405	68.3	91.3
MorphMLP-B	IN-1K	16×3×1	294	67.6	91.3
MorphMLP-B	IN-1K	32×3×1	591	**70.1**	**92.8**

Table 4. Comparisons with the state-of-the-art on Something-Something V2 [22]. Our MorphMLP outperforms previous sota Transformer and CNN methods as a simple backbone without any sophisticated temporal operation.

Method	Pretrain	#Frame	GFLOPs	SSV1 Top-1	SSV1 Top-5
I3D [69]	IN-1K+K400	32×3×2	918	41.6	72.2
NLI3D [69]	IN-1K+K400	32×3×2	1008	44.4	76.0
NLI3D+GCN [69]	IN-1K+K400	32×3×2	1818	46.1	76.8
TSN [66]	IN-1K	8×1×1	33	19.7	46.6
TSM [38]	IN-1K+K400	16×1×1	65	47.2	77.1
TAM [17]	IN-1K	16×1×2	95	48.4	78.8
TANet [43]	IN-1K	16×1×1	66	47.6	77.7
GST [46]	IN-1K	16×1×1	59	48.6	77.9
TEINet [41]	IN-1K	16×1×1	66	49.9	-
SmallBig [35]	IN-1K	16×1×1	105	49.3	79.5
MorphMLP-S	IN-1K	16×1×1	67	50.6	78.0
MorphMLP-S	IN-1K	16×3×1	201	**53.9**	**81.3**

Table 5. Comparisons with the state-of-the-art on Something-Something V1 [22]. Our MorphMLP achieves the best results.

4.2. Video Classification on Kinetics-400

Settings. Kinetics-400 [6] is a large-scale scene-related video benchmark. It contains around 240K training videos and about 20K validation videos in 400 classes. Our code heavily relies on `PySlowFast` [15] repository and the

training recipe mainly follows MViT [16]. We directly load the parameters of `MorphFC` pre-trained on ImageNet and randomly initialize the parameters of $\texttt{MorphFC}_\texttt{t}$ in the video domain. We adopt a dense sampling strategy [68] and AdamW optimizer to train the whole network. The warm-up epoch, total epoch, batch size, base learning rate, and weight decay are 10, 60, 64, 2e-4, and 0.05 respectively. We utilize the same stochastic depth rates in Table 1.

Results. As shown in Table 3, our method achieves outstanding performance with fewer computation costs. Compared with CNN models such as SlowFast [19], our MorphMLP requires 8× fewer GFLOPS but achieves 1.9% accuracy improvement (80.8% *vs*. 79.8%). With only ImageNet-1K pre-training, our method surpasses most of the self-attention based Transformer backbones with large dataset pre-training. For example, compared with ViViT-L [1] pre-trained on ImageNet-21K, our MorphMLP obtains better performance with 20× fewer computations. When our model is scaled larger, the accuracy increases as well. Since the computation cost is relatively low, our method still has great potential for better performance. Such results demonstrate that our MorphMLP is a strong MLP-Like backbone for video recognition.

4.3. Video Classification on Something-Something

Settings. Something-Something [22] is another large-scale dataset, in which the temporal relationship modeling is critical for action understanding. It includes two versions, i.e., V1 and V2, both of which contain plentiful videos over 174 categories. We adopt the same training setting as used for Kinetics-400, except that a random horizontal flip is not applied. We utilize the sparse sampling strategy. The warm-up epoch, total epoch, batch size, base learning rate, and weight decay are 5, 50, 64, 4e-4, and 0.05, respectively. We double the same stochastic depth rates in Table 1.

Results. The comparison results on Something V2&V1 are shown in Table 4 and Table 5 respectively. For SSV2, CNN architectures perform worse than Transformer architectures since they are limited to capturing local spatial and temporal information and struggle to model long-term dependencies. Transformer architectures can achieve better results, but they heavily rely on large-scale dataset pre-training which requires high computation. Compared with CT-Net [34], our MorphMLP can reduce 2.5× computation but achieves 1.2% accuracy gain. Compared with the-state-of-art method MViT [16], which is pre-trained on large video dataset Kinetics-600, our MorphMLP only pre-trained on ImageNet-1K can obtain better performance (70.1% *vs*. 68.7%) with smaller GFLOPS (591G *vs*. 708G). For SSV1, our MorphMLP also achieves outstanding results.

Note that even if we do not add any complicated and unique temporal operation, our simple method can achieve such great performance. This indicates that our model can serve as a strong backbone for further improvement.

Method	Arch	#Param.(M)	mIoU
ResNet50 [24]	CNN	28.5	36.7
PVT-S [67]	Trans	28.2	39.8
Swin-T [40]	Trans	31.9	41.5
GFNet-H-T [50]	FFN	26.6	41.0
CycleMLP-B2 [8]	MLP-Like	30.6	42.4
MorphMLP-T	MLP-Like	26.4	**43.0**
ResNet101 [24]	CNN	47.5	38.8
ResNeXt101-32x4d [73]	CNN	47.1	39.7
PVT-M [67]	Trans	48.0	41.6
GFNet-H-S [50]	FFN	47.5	42.5
CycleMLP-B3 [8]	MLP-Like	42.1	44.5
MorphMLP-S	MLP-Like	41.0	**44.7**
PVT-L [67]	Trans	65.1	42.1
Swin-S [40]	Trans	53.2	45.2
CycleMLP-B4 [8]	MLP-Like	55.6	45.1
MorphMLP-B	MLP-Like	59.3	**45.9**

Table 6. Semantic segmentation on ADE20K [78] val. All models are equipped with Semantic FPN [32].

4.4. Semantic Segmentation on ADE20K

Settings. We conduct semantic segmentation experiments on ADE20K [78], which consists of 20K training images and 2K validation images over 150 semantic categories. Our code is based on `mmsegmentation` [10] toolbox and we follow the experiment setting used in PVT [67]. We simply apply Semantic FPN [32] for fair comparisons, and all the backbones are pre-trained on ImageNet-1K. We adopt AdamW [44] optimizer with cosine learning rate schedule [45], while the initial learning rate is set to 1e-4. The input images are randomly resized and cropped to 512×512 for training, and the shorter sides of images are set to 512 while testing.

Results. The results on ADE20k dataset are shown in Table 6. Our MorphMLP outperforms ResNet [49] and PVT [67] significantly. Compared with Swin-T, our MorphMLP-T can achieve better mIoU (43.0% *vs*. 41.5%) with fewer parameters (26.4M *vs*. 31.9M). Our scaled MorphMLP consistently beats the Swin Transformer [40] as well. Note that compared with GFNet-H-T [50], our MorphMLP-T achieves a slight accuracy gain (81.6% *vs*. 81.3%) on ImageNet-1K but outperforms it significantly on semantic segmentation task (43.0% *vs*. 41.0%), in which short-to-long range information capture pattern plays a critical role.

4.5. Ablation Study

We conduct ablation studies to verify the effectiveness of our design. For Table 7, 8, 9 and 10, we train all the models based on MorphMLP-T for 100 epochs on ImageNet. To explore the variants of our spatial-temporal design, we adopt MorphMLP-S as the backbone for Table 11.

Impact of chunk length. In the MorphMLP, we expand the chunk length gradually. The spatial resolutions of feature maps of Stages 1-4 are 56, 28, 14, 7, respectively.

Stage1	Stage2	Stage3	Stage4	ImageNet Top-1	ADE20K mIoU
56	28	14	7	79.1	41.6
3	3	3	3	78.2	41.0
7	7	7	7	79.0	41.9
14	28	28	7	79.3	42.0
28	28	28	49	79.4	42.3
14	28	28	49	**79.6**	**42.6**

Table 7. Impact of chunk lengths.

#Channels	#Param.(M)	GFLOPs	ImageNet Top-1
C / (2L)	22.0	3.7	78.6
C / L	23.4	4.0	**79.6**
2C / L	28.9	4.6	78.4

Table 8. Dimension of channel groups.

For the horizontal/vertical directions, chunk lengths 14, 28, 28, 49 in Stages1-4 can cover quarter, one, two and all rows/columns of the tokens, respectively, which can progressively capture short-to-long range relations.

As shown in Table 7, there are some alternative ways to set chunk length in each stage. The first line represents that `MorphFC` in each stage covers one row of image tokens, which only models global information, The second and third line utilize the small chunk length, which only captures local structure. The results show that our short-to-long range pattern can perform better than the solely local or global pattern. The reason is that, in the shallow layer, the original spatial texture information of the image is relatively intact. Therefore, it is critical to capture detailed structures in the early stage, especially for downstream tasks, i.e., semantic segmentation, which needs fine grained feature. The features in the deep layers cover more semantic information, thus long-range relation modeling is significant.

Dimension of channel groups. We study the influence of the dimension D for each channel group of `MorphFC`. As shown in Table 8, $D = C/L$ achieves the best trade-off between accuracy and computation.

Detail designs of architecture. We explore the detailed designs of our architecture in Table 9. First, we evaluate the necessity of FC layers from three directions. It shows that each direction plays an important role. Second, we replace the 3×3 convolution with our `MorphFC` layer in ResNet [24] and the result shows that Transformer structure is more suitable for our `MorphFC` than the bottleneck block of CNN. Third, following the ViP [25], we utilize a weighted sum after three directions FC layers. Results show that weighted sum can bring a slight improvement (0.3%).

Comparisons with convolution. We replace the `MorphFC` layer with typical 3×3 and 7×7 convolution to make the comparisons. As shown in Table 10, our `MorphFC` can outperform typical convolution by a large margin. This demonstrates that typical convolution is difficult to capture long-range information, which is crucial to the recognition problem. Furthermore, we adopt two 1D group convolutions along the horizontal and vertical direction, whose kernel sizes are exactly the same as our chunk lengths in each stage. Since convolution is a weight sum operation, it needs to apply padding and sliding overlap window to make input dimension equal to output dimension, which is unnecessary in `MorphFC`. The results in Table 10 show that our method is much better than group conv in terms of speed and accuracy. This indicates the effectiveness of our `MorphFC`.

Dimension	Style	Weight Sum	ImageNet Top-1
H+W+C	Transformer	✔	**79.6**
H+W	Transformer	✔	78.5
H+W+C	CNN	✔	77.2
H+W+C	Transformer	✗	79.3

Table 9. Detailed designs of MorphMLP.

Operation	#Param.(M)	GFLOPs	Throughput (images/s)	ImageNet Top-1
3×3 Conv	34.5	6.2	320	77.3
7×7 Conv	113	20.6	207	77.7
Group Conv	23.4	4.0	305	79.0
Ours	23.4	4.0	418	**79.6**

Table 10. Comparisons with convolution.Throughput is tested on a single V100 GPU with batch size 32.

Method	Order	Standard Residual	Skip Residual	SSV1 Top-1
Parallel	T‖S	✔		49.2
Sequential	T+S	✔		49.8
	S+T	✔		50.2
	T+S		✔	**50.6**
	S+T		✔	31.7

Table 11. Detail designs of MorphMLP block in the video domain.

Detail designs of MorphMLP block in video domain. We explore some alternative designs for our MorphMLP block in the video domain. To begin with, in addition to applying $\texttt{MorphFC}_\texttt{t}$ and `MorphFC` in a sequential way, we can add the features from $\texttt{MorphFC}_\texttt{t}$ and `MorphFC` in parallel. As shown in Table 11, the parallel way performs worse than the sequential way. We argue that it is more difficult for joint spatial and temporal optimization. Moreover, we explore different spatial-temporal orders and residual connections. Standard residual refers to applying a residual connection after each module in MorphMLP block of Fig. 6. Skip residual means that a connection is applied between input features of MorphMLP block and output features of the `MorphFC` (red line in Figure 6). The results show that sequential temporal and spatial order with skip residual connection is the optimal setting.

5. Conclusion

In this paper, we propose a self-attention free, MLP-Like backbone for images and videos, named MorphMLP. MorphMLP is capable of progressively understanding core

details in the images/videos. To our best knowledge, we are the first to apply MLP-Like architecture in the video domain. The experiments demonstrate that self-attention free models can be as strong as and even outperform self-attention based architectures.

Limitations. Through our experiments, we found that the MLP-Like architectures are easier to be over-fitting than CNNs and Vision Transformers. In the future, we will explore more sparse weight connections in MLP-Like structures to alleviate over-fitting. The effects of distillation and pruning on MLP-Like models will be studied.

6. Acknowledgements

This research is supported by the National Research Foundation, Singapore under its NRFF award NRF-NRFF13-2021-0008.

References

[1] A. Arnab, M. Dehghani, G. Heigold, Chen Sun, Mario Lucic, and C. Schmid. Vivit: A video vision transformer. *ArXiv*, abs/2103.15691, 2021. 6, 7

[2] Jimmy Ba, Jamie Ryan Kiros, and Geoffrey E. Hinton. Layer normalization. *ArXiv*, abs/1607.06450, 2016. 4, 5

[3] Gedas Bertasius, Heng Wang, and L. Torresani. Is space-time attention all you need for video understanding? *ArXiv*, abs/2102.05095, 2021. 1, 3, 5, 6

[4] Adrian Bulat, Juan-Manuel Pérez-Rúa, Swathikiran Sudhakaran, Brais Martínez, and Georgios Tzimiropoulos. Space-time mixing attention for video transformer. *ArXiv*, abs/2106.05968, 2021. 6

[5] Nicolas Carion, Francisco Massa, Gabriel Synnaeve, Nicolas Usunier, Alexander Kirillov, and Sergey Zagoruyko. End-to-end object detection with transformers. *ArXiv*, abs/2005.12872, 2020. 3

[6] João Carreira and Andrew Zisserman. Quo vadis, action recognition? a new model and the kinetics dataset. *2017 IEEE Conference on Computer Vision and Pattern Recognition (CVPR)*, pages 4724–4733, 2017. 2, 6

[7] João Carreira and Andrew Zisserman. Quo vadis, action recognition? a new model and the kinetics dataset. *2017 IEEE Conference on Computer Vision and Pattern Recognition (CVPR)*, pages 4724–4733, 2017. 3

[8] Shoufa Chen, Enze Xie, Chongjian Ge, Ding Liang, and Ping Luo. Cyclemlp: A mlp-like architecture for dense prediction. *arXiv preprint arXiv:2107.10224*, 2021. 1, 3, 7

[9] Yunpeng Chen, Yannis Kalantidis, Jianshu Li, Shuicheng Yan, and Jiashi Feng. a^2-nets: Double attention networks, 2018. 1, 3

[10] MMSegmentation Contributors. MMSegmentation: Openmmlab semantic segmentation toolbox and benchmark. https://github.com/open-mmlab/mmsegmentation, 2020. 7

[11] Zihang Dai, Hanxiao Liu, Quoc V. Le, and Mingxing Tan. Coatnet: Marrying convolution and attention for all data sizes. *ArXiv*, abs/2106.04803, 2021. 5

[12] Jia Deng, Wei Dong, Richard Socher, Li-Jia Li, Kai Li, and Li Fei-Fei. Imagenet: A large-scale hierarchical image database. In *2009 IEEE conference on computer vision and pattern recognition*, pages 248–255. Ieee, 2009. 1, 2, 5, 6

[13] Xiaoyi Dong, Jianmin Bao, Dongdong Chen, Weiming Zhang, Nenghai Yu, Lu Yuan, Dong Chen, and B. Guo. Cswin transformer: A general vision transformer backbone with cross-shaped windows. *ArXiv*, abs/2107.00652, 2021. 1, 3

[14] A. Dosovitskiy, L. Beyer, Alexander Kolesnikov, Dirk Weissenborn, Xiaohua Zhai, Thomas Unterthiner, M. Dehghani, Matthias Minderer, G. Heigold, S. Gelly, Jakob Uszkoreit, and N. Houlsby. An image is worth 16x16 words: Transformers for image recognition at scale. *ArXiv*, abs/2010.11929, 2021. 1, 2

[15] Haoqi Fan, Yanghao Li, Bo Xiong, Wan-Yen Lo, and Christoph Feichtenhofer. Pyslowfast. https://github.com/facebookresearch/slowfast, 2020. 6

[16] Haoqi Fan, Bo Xiong, Karttikeya Mangalam, Yanghao Li, Zhicheng Yan, J. Malik, and Christoph Feichtenhofer. Multiscale vision transformers. *ArXiv*, abs/2104.11227, 2021. 3, 6, 7

[17] Quanfu Fan, Chun-Fu Chen, Hilde Kuehne, Marco Pistoia, and David Cox. More is less: Learning efficient video representations by big-little network and depthwise temporal aggregation. *ArXiv*, abs/1912.00869, 2019. 6

[18] Christoph Feichtenhofer. X3d: Expanding architectures for efficient video recognition. *2020 IEEE/CVF Conference on Computer Vision and Pattern Recognition (CVPR)*, pages 200–210, 2020. 6

[19] Christoph Feichtenhofer, Haoqi Fan, Jitendra Malik, and Kaiming He. Slowfast networks for video recognition. *2019 IEEE/CVF International Conference on Computer Vision (ICCV)*, pages 6201–6210, 2019. 3, 6, 7

[20] Peng Gao, Jiasen Lu, Hongsheng Li, R. Mottaghi, and Aniruddha Kembhavi. Container: Context aggregation network. *ArXiv*, abs/2106.01401, 2021. 5

[21] Priya Goyal, Piotr Dollár, Ross B. Girshick, Pieter Noordhuis, Lukasz Wesolowski, Aapo Kyrola, Andrew Tulloch, Yangqing Jia, and Kaiming He. Accurate, large minibatch sgd: Training imagenet in 1 hour. *ArXiv*, abs/1706.02677, 2017. 6

[22] Raghav Goyal, Samira Ebrahimi Kahou, Vincent Michalski, Joanna Materzynska, Susanne Westphal, Heuna Kim, Valentin Haenel, Ingo Fründ, Peter Yianilos, Moritz Mueller-Freitag, Florian Hoppe, Christian Thurau, Ingo Bax, and Roland Memisevic. The "something something" video database for learning and evaluating visual common sense. *2017 IEEE International Conference on Computer Vision (ICCV)*, pages 5843–5851, 2017. 1, 2, 6, 7

[23] Jianyuan Guo, Yehui Tang, Kai Han, Xinghao Chen, Han Wu, Chao Xu, Chang Xu, and Yunhe Wang. Hire-mlp: Vision mlp via hierarchical rearrangement. *arXiv preprint arXiv:2108.13341*, 2021. 3

[24] Kaiming He, X. Zhang, Shaoqing Ren, and Jian Sun. Deep residual learning for image recognition. *2016 IEEE Conference on Computer Vision and Pattern Recognition (CVPR)*, pages 770–778, 2016. 3, 4, 5, 7, 8

[25] Qibin Hou, Zihang Jiang, Li Yuan, Mingg-Ming Cheng, Shuicheng Yan, and Jiashi Feng. Vision permutator: A permutable mlp-like architecture for visual recognition. *ArXiv*, abs/2106.12368, 2021. 1, 2, 3, 5, 6, 8

[26] Andrew G. Howard, Menglong Zhu, Bo Chen, Dmitry Kalenichenko, Weijun Wang, Tobias Weyand, M. Andreetto, and Hartwig Adam. Mobilenets: Efficient convolutional neural networks for mobile vision applications. *ArXiv*, abs/1704.04861, 2017. 3

[27] Jie Hu, Li Shen, Samuel Albanie, Gang Sun, and E. Wu. Squeeze-and-excitation networks. *IEEE Transactions on Pattern Analysis and Machine Intelligence*, 42:2011–2023, 2020. 3

[28] Gao Huang, Zhuang Liu, and Kilian Q. Weinberger. Densely connected convolutional networks. *2017 IEEE Conference on Computer Vision and Pattern Recognition (CVPR)*, pages 2261–2269, 2017. 3

[29] Zilong Huang, Xinggang Wang, Lichao Huang, Chang Huang, Yunchao Wei, and Wenyu Liu. Ccnet: Criss-cross attention for semantic segmentation. In *Proceedings of the IEEE/CVF International Conference on Computer Vision*, pages 603–612, 2019. 1

[30] Boyuan Jiang, Mengmeng Wang, Weihao Gan, Wei Wu, and Junjie Yan. Stm: Spatiotemporal and motion encoding for action recognition. *2019 IEEE International Conference on Computer Vision (ICCV)*, pages 2000–2009, 2019. 6

[31] Youngsaeng Jin, David K. Han, and Hanseok Ko. Trseg: Transformer for semantic segmentation. *Pattern Recognit. Lett.*, 148:29–35, 2021. 3

[32] Alexander Kirillov, Ross Girshick, Kaiming He, and Piotr Dollár. Panoptic feature pyramid networks. In *Proceedings of the IEEE/CVF Conference on Computer Vision and Pattern Recognition*, pages 6399–6408, 2019. 7

[33] Alex Krizhevsky, Ilya Sutskever, and Geoffrey E Hinton. Imagenet classification with deep convolutional neural networks. In F. Pereira, C. J. C. Burges, L. Bottou, and K. Q. Weinberger, editors, *Advances in Neural Information Processing Systems*, volume 25. Curran Associates, Inc., 2012. 3

[34] Kunchang Li, Xianhang Li, Yali Wang, Jun Wang, and Y. Qiao. Ct-net: Channel tensorization network for video classification. *ArXiv*, abs/2106.01603, 2021. 6, 7

[35] X. Li, Yali Wang, Zhipeng Zhou, and Yu Qiao. Smallbignet: Integrating core and contextual views for video classification. *2020 IEEE Conference on Computer Vision and Pattern Recognition (CVPR)*, pages 1089–1098, 2020. 6

[36] Xinyu Li, Yanyi Zhang, Chunhui Liu, Bing Shuai, Yi Zhu, Biagio Brattoli, Hao Chen, Ivan Marsic, and Joseph Tighe. Vidtr: Video transformer without convolutions. *ArXiv*, abs/2104.11746, 2021. 1, 3, 6

[37] Yinong Li, Bin Ji, Xintian Shi, Jianguo Zhang, Bin Kang, and Limin Wang. Tea: Temporal excitation and aggregation for action recognition. *ArXiv*, abs/2004.01398, 2020. 6

[38] Ji Lin, Chuang Gan, and Song Han. Tsm: Temporal shift module for efficient video understanding. *2019 IEEE International Conference on Computer Vision (ICCV)*, pages 7082–7092, 2019. 6

[39] Hanxiao Liu, Zihang Dai, David R. So, and Quoc V. Le. Pay attention to mlps. *ArXiv*, abs/2105.08050, 2021. 1, 3, 5

[40] Ze Liu, Yutong Lin, Yue Cao, Han Hu, Yixuan Wei, Zheng Zhang, S. Lin, and B. Guo. Swin transformer: Hierarchical vision transformer using shifted windows. *ArXiv*, abs/2103.14030, 2021. 1, 3, 5, 6, 7

[41] Zhaoyang Liu, D. Luo, Yabiao Wang, L. Wang, Ying Tai, Chengjie Wang, Jilin Li, Feiyue Huang, and Tong Lu. Teinet: Towards an efficient architecture for video recognition. *ArXiv*, abs/1911.09435, 2020. 6

[42] Ze Liu, Jia Ning, Yue Cao, Yixuan Wei, Zheng Zhang, S. Lin, and Han Hu. Video swin transformer. *ArXiv*, abs/2106.13230, 2021. 1, 3, 6

[43] Zhaoyang Liu, Limin Wang, Wayne Wu, Chen Qian, and Tong Lu. Tam: Temporal adaptive module for video recognition. *ArXiv*, abs/2005.06803, 2020. 6

[44] I. Loshchilov and F. Hutter. Fixing weight decay regularization in adam. *ArXiv*, abs/1711.05101, 2017. 6, 7

[45] Ilya Loshchilov and Frank Hutter. Sgdr: Stochastic gradient descent with warm restarts. *arXiv: Learning*, 2017. 6, 7

[46] Chenxu Luo and Alan L. Yuille. Grouped spatial-temporal aggregation for efficient action recognition. *2019 IEEE International Conference on Computer Vision (ICCV)*, pages 5511–5520, 2019. 6

[47] Daniel Neimark, Omri Bar, Maya Zohar, and Dotan Asselmann. Video transformer network. *ArXiv*, abs/2102.00719, 2021. 1

[48] Mandela Patrick, Dylan Campbell, Yuki M. Asano, Ishan Misra Florian Metze, Christoph Feichtenhofer, A. Vedaldi, and João F. Henriques. Keeping your eye on the ball: Trajectory attention in video transformers. *ArXiv*, abs/2106.05392, 2021. 1, 3, 6

[49] Ilija Radosavovic, Raj Prateek Kosaraju, Ross B. Girshick, Kaiming He, and Piotr Dollár. Designing network design spaces. *2020 IEEE/CVF Conference on Computer Vision and Pattern Recognition (CVPR)*, pages 10425–10433, 2020. 3, 5, 7

[50] Yongming Rao, Wenliang Zhao, Zheng Zhu, Jiwen Lu, and Jie Zhou. Global filter networks for image classification. *ArXiv*, abs/2107.00645, 2021. 7

[51] Mark Sandler, Andrew Howard, Menglong Zhu, Andrey Zhmoginov, and Liang-Chieh Chen. Mobilenetv2: Inverted residuals and linear bottlenecks. In *Proceedings of the IEEE conference on computer vision and pattern recognition*, pages 4510–4520, 2018. 3

[52] Karen Simonyan and Andrew Zisserman. Very deep convolutional networks for large-scale image recognition. *arXiv preprint arXiv:1409.1556*, 2014. 3

[53] A. Srinivas, Tsung-Yi Lin, Niki Parmar, Jonathon Shlens, P. Abbeel, and Ashish Vaswani. Bottleneck transformers for visual recognition. *ArXiv*, abs/2101.11605, 2021. 5

[54] Christian Szegedy, Wei Liu, Yangqing Jia, Pierre Sermanet, Scott Reed, Dragomir Anguelov, Dumitru Erhan, Vincent Vanhoucke, and Andrew Rabinovich. Going deeper with convolutions. In *Proceedings of the IEEE conference on computer vision and pattern recognition*, pages 1–9, 2015. 3

[55] Mingxing Tan and Quoc V. Le. Efficientnet: Rethinking model scaling for convolutional neural networks. *ArXiv*, abs/1905.11946, 2019. 3

[56] Chuanxin Tang, Yucheng Zhao, Guangting Wang, Chong Luo, Wenxuan Xie, and Wenjun Zeng. Sparse mlp for image recognition: Is self-attention really necessary? *arXiv preprint arXiv:2109.05422*, 2021. 3

[57] Ilya O. Tolstikhin, Neil Houlsby, Alexander Kolesnikov, Lucas Beyer, Xiaohua Zhai, Thomas Unterthiner, Jessica Yung, Daniel Keysers, Jakob Uszkoreit, Mario Lucic, and Alexey Dosovitskiy. Mlp-mixer: An all-mlp architecture for vision. *ArXiv*, abs/2105.01601, 2021. 5

[58] Hugo Touvron, Piotr Bojanowski, Mathilde Caron, Matthieu Cord, Alaaeldin El-Nouby, Edouard Grave, Armand Joulin, Gabriel Synnaeve, Jakob Verbeek, and Herv'e J'egou. Resmlp: Feedforward networks for image classification with data-efficient training. *ArXiv*, abs/2105.03404, 2021. 3, 5

[59] Hugo Touvron, M. Cord, M. Douze, Francisco Massa, Alexandre Sablayrolles, and Herv'e J'egou. Training data-efficient image transformers & distillation through attention. In *ICML*, 2021. 5, 6

[60] Du Tran, Lubomir D. Bourdev, Rob Fergus, Lorenzo Torresani, and Manohar Paluri. Learning spatiotemporal features with 3d convolutional networks. *2015 IEEE International Conference on Computer Vision (ICCV)*, pages 4489–4497, 2015. 3

[61] Du Tran, Heng Wang, L. Torresani, and Matt Feiszli. Video classification with channel-separated convolutional networks. *2019 IEEE/CVF International Conference on Computer Vision (ICCV)*, pages 5551–5560, 2019. 6

[62] Du Tran, Hong xiu Wang, Lorenzo Torresani, Jamie Ray, Yann LeCun, and Manohar Paluri. A closer look at spatiotemporal convolutions for action recognition. *2018 IEEE Conference on Computer Vision and Pattern Recognition (CVPR)*, pages 6450–6459, 2018. 3

[63] Ashish Vaswani, Noam M. Shazeer, Niki Parmar, Jakob Uszkoreit, Llion Jones, Aidan N. Gomez, Lukasz Kaiser, and Illia Polosukhin. Attention is all you need. *ArXiv*, abs/1706.03762, 2017. 4, 5

[64] Heng Wang, Du Tran, L. Torresani, and Matt Feiszli. Video modeling with correlation networks. *2020 IEEE/CVF Conference on Computer Vision and Pattern Recognition (CVPR)*, pages 349–358, 2020. 6

[65] Limin Wang, Zhan Tong, Bin Ji, and Gangshan Wu. Tdn: Temporal difference networks for efficient action recognition. *ArXiv*, abs/2012.10071, 2020. 6

[66] L. Wang, Yuanjun Xiong, Zhe Wang, Y. Qiao, D. Lin, X. Tang, and L. Gool. Temporal segment networks: Towards good practices for deep action recognition. In *ECCV*, 2016. 6

[67] Wenhai Wang, Enze Xie, Xiang Li, Deng-Ping Fan, Kaitao Song, Ding Liang, Tong Lu, P. Luo, and L. Shao. Pyramid vision transformer: A versatile backbone for dense prediction without convolutions. *ArXiv*, abs/2102.12122, 2021. 1, 3, 5, 7

[68] X. Wang, Ross B. Girshick, Abhinav Gupta, and Kaiming He. Non-local neural networks. *2018 IEEE/CVF Conference on Computer Vision and Pattern Recognition*, pages 7794–7803, 2018. 1, 3, 7

[69] X. Wang and Abhinav Gupta. Videos as space-time region graphs. In *ECCV*, 2018. 6

[70] B. Wu, Chenfeng Xu, Xiaoliang Dai, Alvin Wan, Peizhao Zhang, M. Tomizuka, K. Keutzer, and Péter Vajda. Visual transformers: Token-based image representation and processing for computer vision. *ArXiv*, abs/2006.03677, 2020. 3

[71] Haiping Wu, Bin Xiao, N. Codella, Mengchen Liu, Xiyang Dai, Lu Yuan, and Lei Zhang. Cvt: Introducing convolutions to vision transformers. *ArXiv*, abs/2103.15808, 2021. 5

[72] Enze Xie, Wenhai Wang, Zhiding Yu, Anima Anandkumar, Jose M Alvarez, and Ping Luo. Segformer: Simple and efficient design for semantic segmentation with transformers. *arXiv preprint arXiv:2105.15203*, 2021. 3

[73] Saining Xie, Ross B. Girshick, Piotr Dollár, Zhuowen Tu, and Kaiming He. Aggregated residual transformations for deep neural networks. *2017 IEEE Conference on Computer Vision and Pattern Recognition (CVPR)*, pages 5987–5995, 2017. 3, 7

[74] Jianwei Yang, Chunyuan Li, Pengchuan Zhang, Xiyang Dai, Bin Xiao, Lu Yuan, and Jianfeng Gao. Focal self-attention for local-global interactions in vision transformers. *arXiv preprint arXiv:2107.00641*, 2021. 3

[75] Tan Yu, Xu Li, Yunfeng Cai, Mingming Sun, and Ping Li. S^2-mlp: Spatial-shift mlp architecture for vision. *arXiv preprint arXiv:2106.07477*, 2021. 3

[76] Li Yuan, Y. Chen, Tao Wang, Weihao Yu, Yujun Shi, Francis E. H. Tay, Jiashi Feng, and Shuicheng Yan. Tokens-to-token vit: Training vision transformers from scratch on imagenet. *ArXiv*, abs/2101.11986, 2021. 1, 3

[77] Hang Zhang, Chongruo Wu, Zhongyue Zhang, Yi Zhu, Haibin Lin, Zhi Zhang, Yue Sun, Tong He, Jonas Mueller, R Manmatha, et al. Resnest: Split-attention networks. *arXiv preprint arXiv:2004.08955*, 2020. 5

[78] Bolei Zhou, Hang Zhao, Xavier Puig, Tete Xiao, Sanja Fidler, Adela Barriuso, and Antonio Torralba. Semantic understanding of scenes through the ade20k dataset. *International Journal of Computer Vision*, 127(3):302–321, 2019. 2, 6, 7

[79] Xizhou Zhu, Weijie Su, Lewei Lu, Bin Li, Xiaogang Wang, and Jifeng Dai. Deformable detr: Deformable transformers for end-to-end object detection. *ArXiv*, abs/2010.04159, 2021. 3

[80] Zhen Zhu, Mengde Xu, Song Bai, Tengteng Huang, and Xiang Bai. Asymmetric non-local neural networks for semantic segmentation. In *Proceedings of the IEEE/CVF International Conference on Computer Vision*, pages 593–602, 2019. 1